



Non-canonical processing of *Arabidopsis* pri-miR319a/b/c generates additional microRNAs to target one RAP2.12 mRNA isoform

Lukasz Sobkowiak¹, Wojciech Karlowski², Artur Jarmolowski¹ and Zofia Szweykowska-Kulinska^{1,2*}

¹ Department of Gene Expression, Faculty of Biology, Institute of Molecular Biology and Biotechnology, Adam Mickiewicz University, Poznan, Poland

² Bioinformatics Laboratory, Faculty of Biology, Institute of Molecular Biology and Biotechnology, Adam Mickiewicz University, Poznan, Poland

Edited by:

Bernie Carroll, The University of Queensland, Australia

Reviewed by:

Hui Wang, Centre for Ecology and Hydrology, Natural Environmental Research Council, UK

Jiayan Wu, Beijing Institute of Genomics, Chinese Academy of Sciences, China

*Correspondence:

Zofia Szweykowska-Kulinska, Department of Gene Expression, Faculty of Biology, Institute of Molecular Biology and Biotechnology, Adam Mickiewicz University, Umultowska 89, 61-614 Poznan, Poland.
e-mail: zofszwey@amu.edu.pl

Arabidopsis miR319a/b/c primary transcripts are unusual due to the presence of a long stem and loop structure containing functional miR319a/b/c molecules. In our experiments carried out using high throughput sequencing (HTS), we have shown that additional microRNAs (miRNAs), miR319a.2/b.2/c.2 are generated from the upper part of the same hairpin structure. We have also found cognate miRNAs.2*/b.2*/c.2* to be present in the HTS results with a considerably lower number of reads. Northern hybridization revealed that miR319b.2 is mainly expressed in 35-day-old plant rosette leaves, as well as in stem and inflorescences of 42- and 53-day-old plants. Moreover, it carries multiple signatures of a functional miRNA, including as follows: (i) its biogenesis is HYL1-dependent; (ii) it is incorporated in a substantial amount into RISC complexes containing AGO1, AGO2, or AGO4 protein; (iii) 24 nt-long species of miR319b.2 have been found in inflorescences to be more abundant than 21 nt miR319b.2 species; (iv) it is present in various ratios to miR319b during plant development, which suggests the existence of a regulatory mechanism responsible for its biogenesis/processing; (v) there is an observed cross-species conservation of the miR319a/b/c stem nucleotide sequence extending beyond mature miRNA region; and (vi) all evidence suggests that intron-containing RAP2.12 mRNA isoform is the target for miR319b.2. All these features prompt us to claim miR319b.2 as a functional miRNA molecule.

Keywords: miRNA, pri-miRNA, RAP2.12, splicing, gene expression

INTRODUCTION

MicroRNAs (miRNAs) represent a class of endogenous, 21–24 nt-long regulatory RNA molecules (Llave et al., 2002; Reinhart et al., 2002; Palatnik et al., 2003). They are involved in the regulation of gene expression by targeting the cognate mRNA molecules for cleavage, or by inhibiting their translation. In *Arabidopsis thaliana* plants, the mature miRNAs are generated from the fold-back hairpin-like structure of nuclear-localized *MIR* gene transcripts termed pri-miRNAs. At least eight proteins are involved in plant miRNA precursor's maturation process: type-III ribonuclease DICER-LIKE 1 (DCL1), dsRNA binding protein HYPONASTIC LEAVES 1 (HYL1, DRB1), zinc-finger protein SERRATE (SE), forkhead-associated (FHA) domain-containing protein DAWDLE (DDL), CAP BINDING PROTEIN 20 (CBP20), CAP BINDING PROTEIN 80 (CBP80/ABH1), methyltransferase HUA ENHANCER 1 (HEN1), and HASTY – an ortholog of animal Exportin 5 (Park et al., 2002, 2005; Han et al., 2004; Kurihara and Watanabe, 2004; Vazquez et al., 2004; Lobbes et al., 2006; Yang et al., 2006b,a; Kim et al., 2008; Laubinger et al., 2008; Yu et al., 2008; Huang et al., 2009).

Plant miR159 and miR319 genes are highly conserved and their representatives can be found in a variety of plants from mosses to flowering plants (Kozomara and Griffiths-Jones, 2011). It is postulated that miR159 and miR319 evolved from a common

ancestor and share sequence identity in 17 out of 21 nt (Kozomara and Griffiths-Jones, 2011; Li et al., 2011). However, due to sequence specificity and temporal and special expression patterns in *Arabidopsis* plants, they have distinct targets; miR159 downregulates the expression of MYB, while miR319 downregulates the expression of TCP transcription factor, respectively. The miR159 is involved in flowering, male fertility, and ABA-dependent seed germination processes, while miR319 plays a role in leaf and flower development; thus, both are critical for plant development, growth, morphogenesis, and reproduction (Palatnik et al., 2007; Reyes and Chua, 2007; Nag et al., 2009). Both *MIR159* and *MIR319* families contain three genes: *MIR159a/b/c*, and *MIR319a/b/c*, respectively. A unique feature of *MIR159* and *MIR319* genes is the presence of a long stem and loop structure. The base-proximal segment of miR159/319 stem and loop precursors is conserved, while the loop-proximal part is conserved to a lesser extent (Bologna et al., 2009). The biogenesis pathway of both miRNAs is unusual since it is a loop-to-base processing mechanism that begins with the cleavage of the loop, instead of the usual cut at the base of the stem-loop structure. Moreover, in several cases, additional small RNAs generated from miRNA 319a/b/c precursors were observed. It is possible that a non-canonical mechanism of the miRNA159/319 maturation potentially generates additional sRNAs from pri-miRNA159/319

hairpins. These additional sRNAs may be non-functional intermediates generated during the miRNA biogenesis pathway or functional, regulatory RNA molecules (Addo-Quaye et al., 2009; Bologna et al., 2009). It was shown by Zhang et al. (2010) that additional sRNAs generated from miR159a, miR319a, and miR319b precursors are stable in *A. thaliana* plants infected by various *Pseudomonas syringae* strains. They have shown that miR319b.2 is the main sRNA molecule derived from pri-miRNA319b. In this paper, we show that miR319b.2 sRNA is also present at a relatively high level in *Arabidopsis* stems and inflorescences in non-infected plants. Moreover, our analysis shows that these additional small RNAs exhibit many features similar to functional miRNA molecules, namely, they are associated with AGO proteins, and our results point to an intron-containing RAP2.12 mRNA isoform as a target of these miRNAs.

MATERIALS AND METHODS

PLANT MATERIAL AND GROWTH CONDITIONS

Arabidopsis thaliana (L.) Heynh, Col-0 wild type plants, homozygous *se-1* plants (NASC, N3257), homozygous T-DNA insertion line *hyl1-2* (SALK_064863), homozygous line Δ *miR319b* (SALK_037093), and *miR319boe* (SALK_059451) were grown in conditions as described in (Szarzynska et al., 2009). Plants for developmental and organ specific northern blot analyses and developmental quantitative real-time PCR profiling of pri-miRNAs from *MIR319* family were grown in the hydroponic growing system for *A. thaliana* (Araponics SA, Liege, Belgium).

RNA ISOLATION

For northern blot analyses, total RNA was isolated from 14-day-old seedlings, 20-day-old plants, and from organs (roots, rosette leaves, stems, and inflorescences) collected in 35, 42, and 53 days after sowing (DAS), using the method described in (Pant et al., 2009). For quantitative real-time PCR analyses, total RNA was isolated as described in (Szarzynska et al., 2009).

DEEP SEQUENCING OF RNA AND BIOINFORMATIC ANALYSES

Total RNA isolated from the wild type *A. thaliana* Col-0 35-day-old rosette leaves (plants were grown in soil) was used for a small RNA library construction. The small RNA libraries were generated and sequenced by Illumina (Fasteris SA, Plan-les-Ouates, Switzerland and British Columbia Cancer Agency, Vancouver, BC, Canada). Adaptor sequences were identified and trimmed from each read using a customized Perl script. Reads in which the adaptor could not be identified were discarded. Two independent rounds of sequencing resulted in a total of more than five million unique, quality-filtered, and adaptor-trimmed reads. As expected for a sRNA sequencing procedure, the size distribution of the short sequences revealed the presence of dominating classes of 24 and 21 nt reads. The maximum read count in our sample was 657050. A BWA program was used to align the trimmed reads to the set of pri-miRNAs and miRNA genes (Li and Durbin, 2010). For each library, we counted the number of trimmed reads within the 18–24 nt range. Reads with counts of less than 5 were discarded giving final number of 41829 and 167616 sequences for two separate replicas.

Counts for the sequences which were mapping to the pri-miRNA were normalized by the total number of 18–24 nt trimmed

reads in the library and presented in the form of “reads per million (RPM)”. Trimmed reads that were <18 nt or >24 nt were not considered in this analysis. Three libraries were downloaded from the GEO database: GSM253622, GSM253623, and GSM253624, representing the sequences immunopurified with AGO1, AGO2, and AGO4 complexes, respectively. The reads were mapped to pri-miRNA with the BWA program.

The data discussed in this publication have been deposited in NCBI's Gene Expression Omnibus and are accessible through GEO Series accession number GSE35335¹.

NORTHERN BLOT ANALYSES

RNA (30–50 μ g) was fractionated on a 15–17% denaturing (7 M urea, Sigma, Deisenhofen, Germany) polyacrylamide gel (PAGE), transferred to a Hybond-NX membrane (Amersham Biosciences-GE Healthcare, Little Chalfont, UK) by capillary transfer, using 20xSSC buffer, and fixed by UV-crosslinking. Pre-hybridization was carried out at 42°C for 2 \times 30 min, using PerfectHyb Hybridization Buffer (Sigma, Deisenhofen, Germany). Probes were labeled with γ ³²P ATP (6000 Ci/mmol; NEN-PerkinElmer Life and Analytical Sciences, Waltham, MA, USA), using T4 polynucleotide kinase (Roche, Mannheim, Germany) and purified on Illustra Micro Spin G-25 Columns (GE Healthcare). Hybridization was performed overnight at 42°C. Lengths of RNA molecules were estimated using ³²P-labeled Decade Marker System (Ambion). Oligonucleotides complementary to miR159/319 and miR319b.2 (see **Table A1** in Appendix) were used as probes. A probe complementary to U6 snRNA was used as a loading control.

SEMIQUANTITATIVE ANALYSIS OF pri-miRNA319b EXPRESSION

The concentration of cDNA from the wild type, *miR319boe* and Δ *miR319b* mutant plants was normalized against the β -actin as described in (Szarzynska et al., 2009). The PCR products were electrophoresed on 1.2% agarose gels in 1 \times TBE buffer (for primer sequences see **Table A1** in Appendix).

QUANTITATIVE REAL-TIME PCR PROFILING OF pri-miRNAs AND RAP2.12 mRNA

Real-time PCR analyses were carried out using methodology described in (Szarzynska et al., 2009). Log₁₀ were calculated from the fold change of particular pri-miRNAs or RAP2.12 mRNA to PP2A transcript (At1g69960).

5'-RACE EXPERIMENTS

5'-RACE experiments were performed using SMARTer RACE cDNA Amplification Kit (Clontech, Mountain View, CA, USA), according to the manufacturer's protocol. All primers used in the experiments are listed in **Table A1**.

RESULTS

DEEP SEQUENCING REVEALS THE PRESENCE OF ADDITIONAL SMALL RNAs GENERATED FROM pri-miRNA319 PRECURSORS

We carried out SOLEXA sequencing reactions of RNA enriched with small RNAs isolated from 35-day-old *A. thaliana* rosette

¹<http://www.ncbi.nlm.nih.gov/geo/query/acc.cgi?acc=GSE35335>

leaves. As already reported by Bologna et al. (2009) and Zhang et al. (2010), we also found extra sRNA species generated from the same stem and loop structure where miRNA 319a/b/c and miRNAa*/b*/c* are embedded. They are located in the loop-proximal part of the stem and loop precursor structure (Figure 1). These most abundant species were named miRNA 319a.2/319b.2/319c.2, respectively. We also found sRNA species that can be regarded as miRNA* to miRNA 319a.2/b.2. Table 1 shows normalized counts for the reads of the miRNAs derived from 319a/b/c precursors found in SOLEXA deep sequencing results. File A1 in Appendix contains the full list of all matching sRNAs, which originate from pri-miR319a/b/c. Analysis of these data clearly shows that the number of reads for miR319b.2 is the highest, even exceeding the number of the reads obtained for miR319a/b, miR319a, and miR319b are identical in sequence; therefore, it is not feasible to distinguish the number of reads derived from each locus separately.

QUANTITATIVE REAL-TIME PCR PROFILING OF pri-miRNAs FROM *MIR319* FAMILY AT DIFFERENT DEVELOPMENTAL STAGES IN WILD TYPE *A. THALIANA* PLANTS

The small number of reads for miR319c, miR319c.2, and miR319a.2 obtained in the SOLEXA experiments induced us to evaluate the expression profiles of all *MIR319* family members in various developmental stages and organs studied.

We designed primers to specifically amplify each of the particular *MIR319* gene family transcripts, and using real-time PCR, we carried out pri-miR319a/b/c expression profiling. Figure 2 shows the obtained results. All family members show differences at the transcript level during plant development. For instance, pri-miR319c expression decreases, while pri-miR319a and pri-miR319b increase in roots of 42-day-old plants as compared to their level in 35- and 53-day-old plants, respectively. We were not able to detect pri-miR319a in rosette leaves of 42- and 53-day-old plants, while at the same time, we observed the expression of two other family members with the highest level of pri-miR319c. The levels of all pri-miRs319 differ in rosette leaves of 35-day-old plants. Pri-miR319b and pri-miR319c are almost to the same level. However, our high throughput sequencing (HTS) results do not show the same amount of mature miR319a/b and miR319c in rosette leaves of the 35-day-old plants. It indicates that the level of

pri-miR does not necessarily mirror the level of mature miRNA. Generally, the highest expression of all *MIR319* family genes occurs in stems and inflorescences. Our real-time PCR data shows that pri-miR319b from the *MIR319* family is the dominating transcript present in the majority of tissues studied.

MIR319b OVEREXPRESSION AND NULL MUTANTS SHOW PHENOTYPIC DIFFERENCES IN COMPARISON TO WILD TYPE PLANTS

We identified a null-insertional T-DNA *Arabidopsis* mutant in the *MIR319b* locus (SALK_037093; Δ miR319b), and a *MIR319b* overexpression mutant (Salk_059451; *miR319boe*) within SALK collection. Both of them showed phenotypic differences when compared to wild type plants (Figure 3A). To our surprise, both mutants exhibited growth retardation. However, the retardation is more profound in the case of the overexpression mutant. Also, the shape of rosette leaves is changed when compared to wild type plants. Leaves of the null mutant plant are narrower, their margins are rolled inwards, while the morphological changes in the case of the plant overexpressing *MIR319b* are more profound, showing a more compact rosette of arrow-shaped leaves, leaf serrated margin, its blade sharply pointed at the tip, and a strong leaf curvature when compared to wt plants. We did not observe any differences in flower shape and structure. In general, the phenotype of the *miR319boe* mutant resembles strongly the phenotype of *MIR-JAW* (*MIR319a*) overexpressing mutant described by Weigel et al. (2000). RT-PCR reaction carried out using RNA isolated from 42-day-old stems for *MIR319b* transcript detection revealed the increased level of primary transcript in the *miR319boe* mutant and the lack of transcript in the case of Δ miR319b mutant plants (Figure 3B). Northern hybridization shows the lack of miR319b.2 in the null mutant plants and increased levels of miR319a/b/c and miR319b.2 in the *miR319boe* mutant, as compared to wild plants. The very faint hybridization signal observed in the case of the Δ miR319b mutant, when the radioactive probe for miR319b.2 was used, derives probably from the weak expression of miR319a.2 that may weakly cross-hybridize (there are two mismatches between miR319a.2 and miR319b.2, Figures 3C,D). Since there are 4 nt mismatches between miR319b.2/miR319c.2 and five between miR319a.2/miR319c.2, we anticipate it to be unlikely that the probe for miR319b.2 detection is cross-hybridizing with the miR319c.2. Northern hybridization results are in agreement with

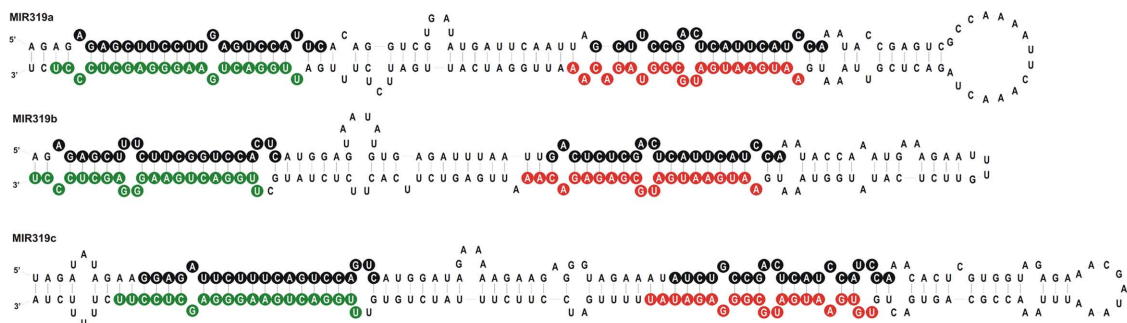


FIGURE 1 | Stem and loop structures of *Arabidopsis* pre-miR319 precursors. Sequences of miR319a, b, and c are in green, sequences representing miRNA319a.2, b.2, and c.2 are in red, and star sequences are in black circles, respectively.

Table 1 | Number of representative reads for specific miR319 species and additional miRNAs generated from their precursors.

| Micro RNA species | Counts (RPM) |
|------------------------|--------------|
| miR319a/b ¹ | 157 |
| miR319a* | 0 |
| miR319a.2 | 13 |
| miR319a.2* | 6 |
| miR319b/a ¹ | 157 |
| miR319b* | 171 |
| miR319b.2 | 889 |
| miR319b.2* | 16 |
| miR319c | 53 |
| miR319c* | 0 |
| miR319c.2 | 13 |
| miR319c.2* | 0 |

The RPM counts were rounded to the nearest integer value.

¹miR 319a and miR 319b are identical in sequence; therefore, it is not possible to distinguish the number of reads derived from each locus separately.

the expression profile of pri-miR319a/b/c described in previous chapter (see **Figure 2**). All these observations, together with the deep sequencing data, suggest that miR319b.2 represents a stable molecule being a product of pre-miR319b processing.

miRNA 319b.2 DERIVED FROM pri-miR319b HAS PROPERTIES OF FUNCTIONAL microRNA

The inspection of the GEO database of the HTS results for AGO1, AGO2, and AGO4 immunoprecipitates for miR319a/b, miR319c, and miR319a.2/b.2/c.2 revealed the highest number of reads for miRNA 319a/b and miR319b.2 as RNA species incorporated into RISC complexes. This suggests a functional role for miR319b.2². **Table 2** shows the numbers of particular miRNAs and miRNAs from the miR319 family found in AGO1, AGO2, and AGO4 immunoprecipitates. Zhang et al. (2010) have recently shown the presence of miR319a.2, as well as miR319b.2, in small RNA libraries from *Arabidopsis* infected with various *P. syringae* pv. tomato (Pst) DC3000 strains, which again strengthens the idea that these miRNAs may be functional.

We studied the presence of miR319b.2 in plants by carrying out northern hybridization for miR159/319 and miR319b.2 in selected developmental stages and organs (see **Figure 4**). Because of high similarity between miR159 and miR319 families that share sequence identity of 17 out of 21 nt, both species hybridize to miR319a/b probe. Since in the $\Delta miR319b$ mutant background only a very faint hybridization signal for miR319a.2 was observed (**Figure 3**), we omitted *MIR319a* and *MIR319c* expression in miR319b/miR319b.2 ratio calculations. Analysis of hybridization signals shows that miR159/319b and miR319b.2 are detectable predominantly in rosette leaves, stems, and inflorescences (**Figures 4C–E**). The ratio of hybridization signals for miR319b to miR319b.2 in stems shows a non-equimolar abundance of both micro RNAs, with three times higher abundance

of miR319b in 35-day-old and 42-day-old plants. However, in 53-day-old stems this ratio is changed and shows only 1.7 higher expression of miR319b in comparison to miR319b.2. Interestingly, the amount of miR319b.2 in 35-day-old rosette leaves exceeds the amount of miR319b (**Figure 4C**). It is in agreement with our HTS data that shows a substantially higher number of miR319b.2 reads than that of miR 319a/b. Changes in stoichiometry between miR319b and miR319b.2, and the higher amount of the miR319b.2 in comparison to miR319b in 35-day-old rosette leaves supports our idea of a possible functional and regulatory role of miR319b.2.

In 42-day-old and 53-day-old inflorescences we observed (in addition to 21 nt long miR319b.2) 24 nt-long species, which constitute the main hybridization band (**Figures 4D,E**). The 24 nt-long miRNA species have already been reported and represent the products of DCL3 activity (Vazquez et al., 2008; Zhou et al., 2010). Moreover, it was shown by Vazquez et al. (2008), that 24 nt-long miRNA species are present predominantly in the inflorescences. The observed 24 nt length of miR319b.2 in inflorescences emphasizes its miRNA-like biogenesis and characteristics specific of miRNA species.

It was shown that the biogenesis of the miR319b is HYL1-dependent (Feijie and Yuke, 2007; Szarynska et al., 2009). Therefore, we tested whether the amount of mature miR319b.2 also depended on the activity of the HYL1 protein. **Figure 4F** shows that, indeed, the accumulation of miR319b.2 is decreased in the *hyl1-2* mutant, and the same was observed for the miR159/319. Thus we concluded that the biogenesis of both miR319b.2 and miR319b is HYL1-dependent.

RAP2.12 mRNA AS A TARGET FOR miR319b.2

A bioinformatic search of putative miR319b.2 targets pointed to five mRNAs (see **Table A2** in Appendix). One of them was the At1g53910 gene encoding RAP2.12, a member of the ERF (ethylene response factor) subfamily B-2 of ERF/AP2 transcription factors family. **Figure 5** shows the structure of *RAP2.12* gene and its two mRNA isoforms. There are two alternatively spliced mRNA isoforms. One of them is fully spliced, while the other retains a second intron, which is located within the 3'-UTR. As shown in **Figures 6A,B**, real-time PCR measurements revealed an approximately ninefold higher amount of RAP2.12 mRNA isoform containing intron in comparison to the one that is fully spliced; both in 42-day-old wild type plant stems and inflorescences (**Figures 6A,B**). Only RAP2.12 mRNA isoform containing intron can be targeted by miR319b.2 within 3'-UTR region (**Figure 5B**). In the NEOMORPH database³, there are RAP2.12 mRNA fragments which are cut exactly at the putative slicing site, which is located in the middle of the intron. However, using the 5'-RACE approach we were not able to prove experimentally that RAP2.12 mRNA intron-containing isoform is cleaved by miR319b.2-guided RISC complex at the exactly predicted site. Our 5'-RACE results show mRNA fragments cut close, and always downstream from the putative slicing site (**Figure 5B**). We decided to compare the amount of putative 3'-intron-containing RAP2.12 mRNA isoform cleavage product in wt plants, *miR319b*oe, and $\Delta miR319b$ mutant

²<http://www.ncbi.nlm.nih.gov/geo/>

³<http://neomorph.salk.edu/aj/pages/smRNAome.html>

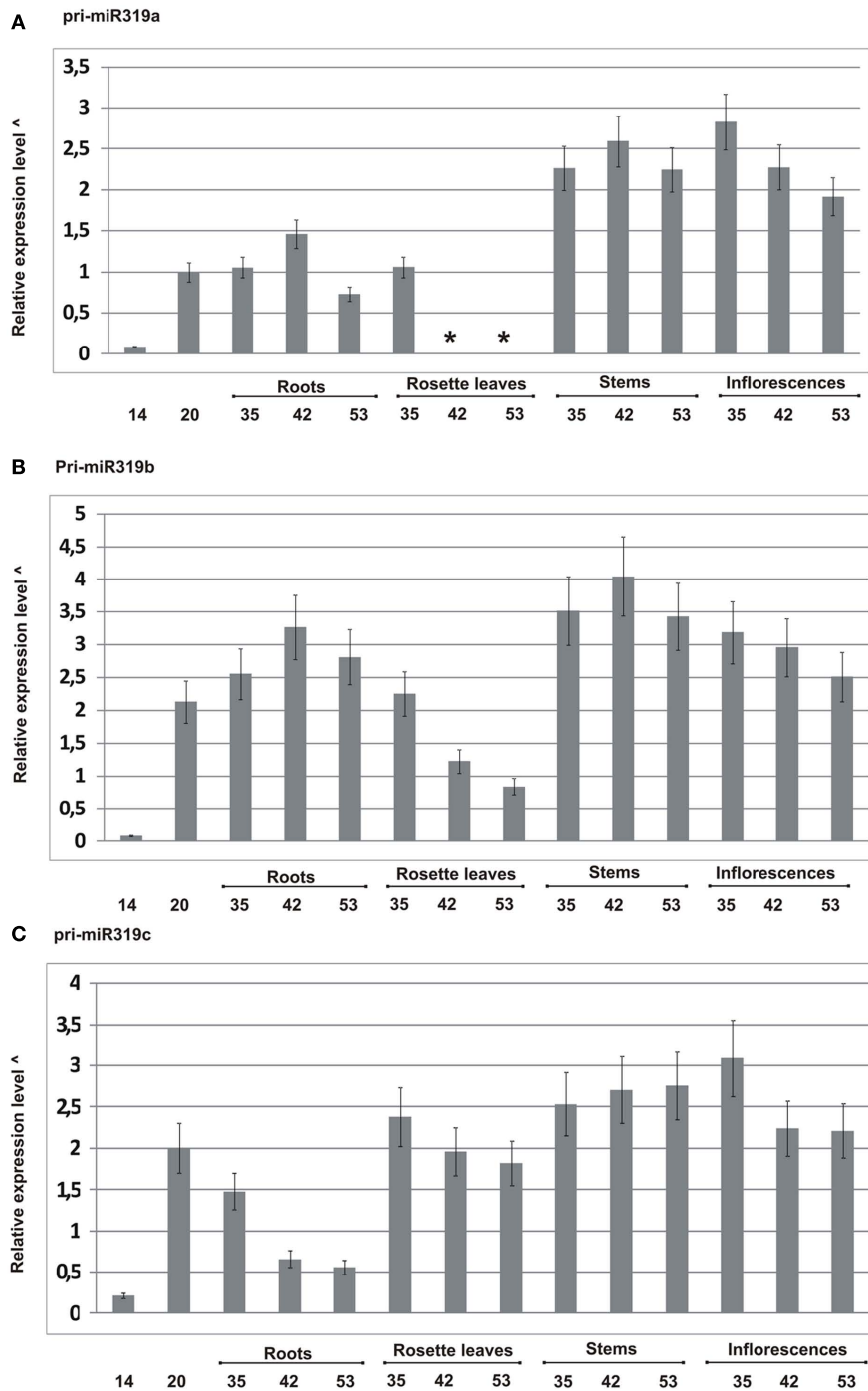


FIGURE 2 | Quantitative real-time PCR profiling of pri-miRNAs from MIR319 family in different developmental stages in wild type *A. thaliana* plants (14-, 20-, 35-, 42-, and 53-day-old plants). (A–C)

Expression patterns of pri-miR319a, pri-miR319b, and pri-miR319c, respectively. *Not detected. $^{\wedge}\log_{10}$ calculated from the fold change of particular pri-miRNAs standardized to the PP2A transcript level (At1g69960). Because the expression of pri-miR319a/b/c is in most cases

lower than the level of PP2A transcript, the graph was rescaled according to the following formula: $\text{abs}(x_{\text{max}} - x)$, where abs denotes absolute value, x_{max} represents the lowest integer value of relative expression level in the original graph and x represents actual expression level for a given pri-miRNA in the particular developmental stage. Real-time PCR for all pri-miR319 was carried out in three biological replicates. Thin black lines represent SD.

plants. Agarose gel electrophoresis of 5'-RACE product revealed almost no product in the $\Delta miR319b$ mutant background, while

it was present in higher amounts in the *miR319boe* mutant background as compared with the wild type plants (Figure 5C). Apart

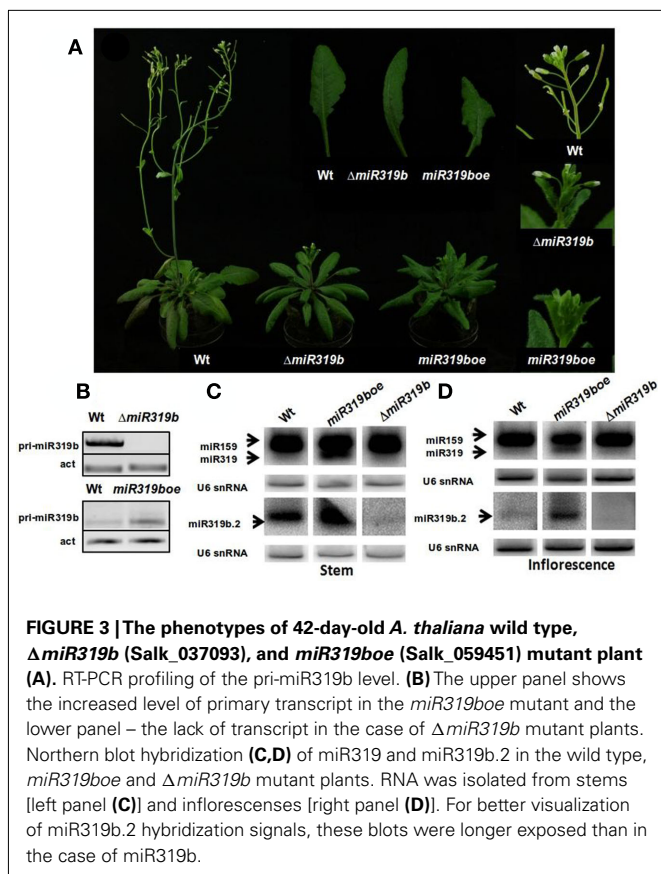


Table 2 | Detection of miR319 a/b/c and additional sRNAs from miR319a/b/c precursors within AGO1, AGO2, and AGO4 immunoprecipitates.

| miRNA | AGO1 | AGO2 | AGO4 |
|-----------|------|------|-------------|
| miR319a/b | 705 | 80 | 167 |
| miR319a.2 | 0 | 0 | 92 (23 nt) |
| miR319b.2 | 206 | 75 | 206 (23 nt) |
| miR319c | 16 | 0 | 32 |
| miR319c.2 | 42 | 0 | 1 |

from the 5'-RACE slicing product of the expected length, we also observed degradation products (marked with a star in **Figure 5C**) that are present only in wt and *miR319boe* mutant lines.

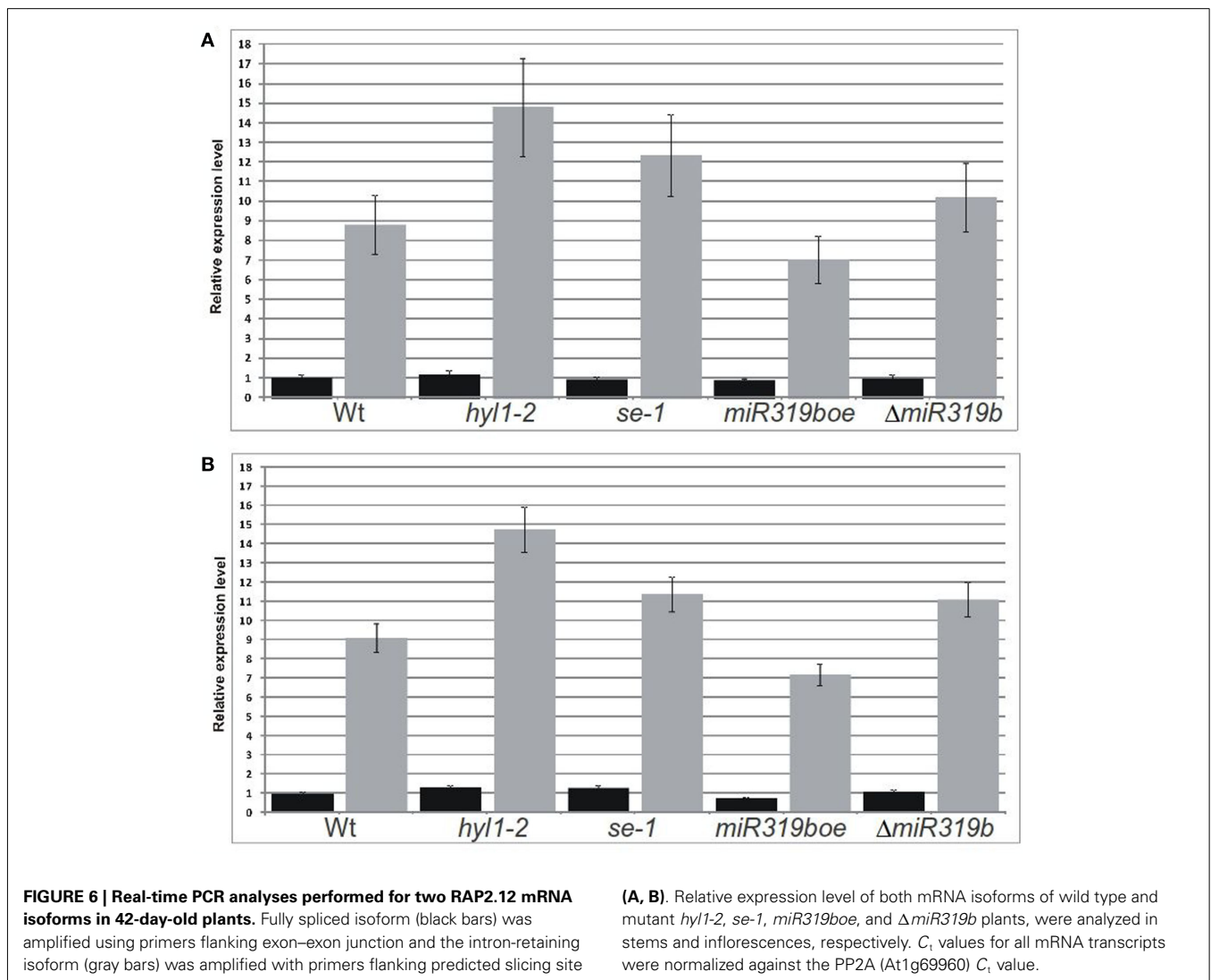
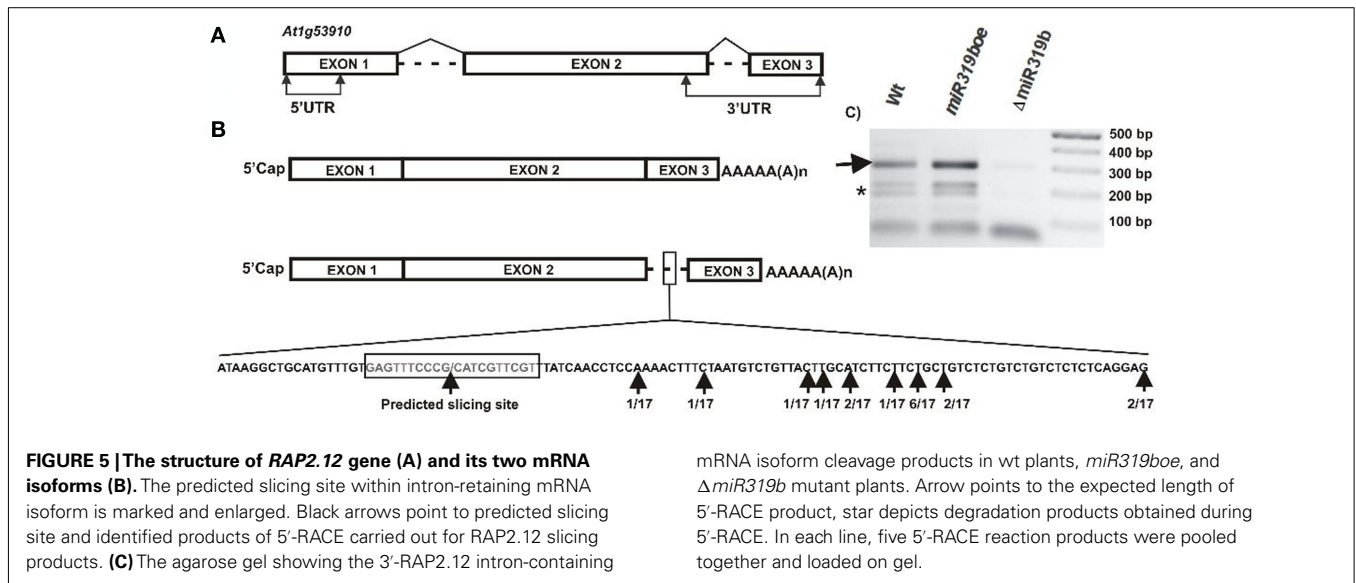
The real-time PCR was performed using primers flanking the predicted slicing site for five putative miR319b.2 targets in wt plants and *hyll-2*, *se-1*, *miR319boe*, and $\Delta miR319b$ mutants, respectively. The experiments were done for 42-day-old plants and RNA was isolated from stems and inflorescences. Only in the case of RAP2.12 we observed the expected results. For the intron-retaining mRNA isoform, the level in *hyll-2*, *se-1*, and $\Delta miR319b$ mutants was increased, while in the *miR319boe* mutant – decreased, when compared to *Arabidopsis* wt plants (**Figures 6A,B**). In parallel experiments, no significant changes were observed in case of the fully spliced RAP2.12 mRNA isoform

(**Figures 6A,B**). All these results indicate that RAP2.12 may be a target for miR319b.2 in stem and inflorescences of *A. thaliana* plants.

DISCUSSION

Recent bioinformatic analyses of eukaryotic transcriptome sequences generated using new generation sequencing (NGS) approaches revealed the presence of multiple types of small RNA species with known and unknown functions (Sobala and Hutvagner, 2011). Studies carried out on *Arabidopsis* transcriptome revealed the presence of a new class 19 nt-long small RNAs corresponding to the 5' end of the specific tRNA species. These small RNAs accumulate to high levels in phosphate-starved roots. However, their biological function is still not clear (Hsieh et al., 2010). In addition, it was found that small RNAs with evolutionary conservation of size and position are derived from the vast majority of snoRNA loci in *Arabidopsis*, as well as in other species. These sno-derived RNAs (sdrRNAs) are associated with *Arabidopsis* AGO7. It is postulated that there is an interplay between the RNA silencing and snoRNA-mediated RNA processing and RNA-directed regulatory system (Taft et al., 2009). In humans, many small RNAs derived mainly from 3'-ends of intron sequences and 3'-UTRs were reported. They were found to be associated with AGO1/2. Valen et al. (2011) revealed that these sRNAs are the products of non-canonical miRNA biogenesis pathways. Finally, it was shown that viral infection by rice stripe virus (RSV) induces expression of novel-phased miRNAs and the accumulation of miRNA*s from rice conserved cellular miRNA precursors (Du et al., 2011). All of these data show that we experience the genesis of the still-expanding realm of small regulatory RNAs deriving from the known, canonical RNA species.

Our studies regarding miR319b.2 indicate that new, functional sRNA molecules are generated from already known, conservative *Arabidopsis* miRNA genes. As mentioned previously, Zhang et al. (2010) have shown the presence of miR319a.2 and miR319b.2 in small RNA libraries from *Arabidopsis* infected with various *P. syringae* pv. tomato (Pst) DC3000 strains. However, our results show that it is mainly miR319b.2, which is expressed during plant development in non-stressed conditions. We cannot rule out the possibility that miR319a.2 and miR319c.2 are generated at higher levels in other developmental stages than the ones we studied, or in a plants response to stress conditions. In this paper, we show that miR319b.2 derived from pri-miR319b has properties of many functional miRNAs, such as: (i) its biogenesis is HYL1-dependent; (ii) it is incorporated in a substantial amount into RISC complexes containing AGO1, AGO2, or AGO4 proteins; (iii) 24 nt-long species of miR319b.2 have been found in inflorescences, where they are more abundant than 21 nt-long miR319b.2 species (Vazquez et al., 2008; Hu et al., 2011); (iv) it is present in various ratios to miR319b during plant development, which suggests the existence of a regulatory mechanism responsible for its biogenesis/processing; (v) there is cross-species conservation of the miR319a/b/c stem nucleotide sequence extending beyond the mature miRNA region. This conservation is clearly visible in the regions where miR319a.2/b.2/c.2 are located. Although this conservation is not as pronounced as in the case of the mature miR319a/b/c sequences, one can observe a clustering of these



of intron-retained RAP2.12 isoform in the $\Delta miR319b$ mutant plants to be higher than in the wild type plants and at least the same as in the case of *hyl1-2* or *se-1* mutants. The level of the RAP2.12 intron-retained isoform is higher than that in the wild type plants, but it does not reach the level of this isoform observed for miRNA biogenesis mutants. We anticipate that the low levels of miR319a.2 and miR319c.2 still present in the $\Delta miR319b$ mutant plants may be responsible for targeting the RAP2.12 intron-retained isoform and down-regulating its expression, in comparison to *hyl1-2* or *se-1* mutants in which the biogenesis of all of these miRNAs is affected. This prediction is also supported by the very weak presence of the slicing product in the $\Delta miR319b$ mutant plants that can be the result of miR319a.2 and/or miR319c.2 activities.

The miR319a/b/c-targeting of the TCP transcription factors was shown in jasmonate biosynthesis, which is involved in plant senescence (Schommer et al., 2008). RAP2.12 with one alternatively spliced mRNA isoform is potentially targeted by

miR319b.2 and is also involved in plant senescence and plant response to osmotic stress (Papdi et al., 2008). Thus, it is feasible that both types of miRNAs: miR319a/b/c and miR319a.2/b.2/c.2 are involved in a similar physiological processes in plant development.

ACKNOWLEDGMENTS

This study was supported financially with a grant awarded by the Ministry of Higher Education and Sciences, Poland (NN301301137); Ph.D. grant awarded by the Ministry of Higher Education and Sciences, Poland (NN301035839 to Lukasz Sobkowiak and Zofia Szweykowska-Kulinska); a grant for scientific research from the Dean of Biology Faculty, Adam Mickiewicz University, Poznan, Poland, and European Funds, Human Capital Operation Program 8.2.2, Poznan (to Lukasz Sobkowiak). We thank Prof. Ewa Czarnecka-Verner for a critical review of this manuscript and Lance Verner for proof reading.

REFERENCES

- Addo-Quaye, C., Snyder, J. A., Park, Y. B., Li, Y. F., Sunkar, R., and Axtell, M. J. (2009). Sliced microRNA targets and precise loop-first processing of MIR319 hairpins revealed by analysis of the *Physcomitrella patens* degradome. *RNA* 15, 2112–2121.
- Bologna, N. G., Mateos, J. L., Bresso, E. G., and Palatnik, J. F. (2009). A loop-to-base processing mechanism underlies the biogenesis of plant microRNAs miR319 and miR159. *EMBO J.* 28, 3646–3656.
- Du, P., Wu, J., Zhang, J., Zhao, S., Zheng, H., Gao, G., Wei, L., and Li, Y. (2011). Viral infection induces expression of novel phased microRNAs from conserved cellular microRNA precursors. *PLoS Pathog.* 7, e1002176. doi:10.1371/journal.ppat.1002176
- Feijie, W., and Yuke, H. (2007). The N-terminal double-stranded RNA binding domains of *Arabidopsis* HYPONASTIC LEAVES 1 are sufficient for pre-microRNA processing. *Plant Cell* 19, 914–925.
- Han, M. H., Goud, S., Song, L., and Fedoroff, N. (2004). The *Arabidopsis* double-stranded RNA-binding protein HYL1 plays a role in microRNA-mediated gene regulation. *Proc. Natl. Acad. Sci. U.S.A.* 101, 1093–1098.
- Hsieh, L. C., Lin, S. I., Kuo, H. F., and Chiou, T. J. (2010). Abundance of tRNA-derived small RNAs in phosphate-starved *Arabidopsis* roots. *Plant Signal. Behav.* 5, 537–539.
- Hu, Q., Hollunder, J., Niehl, A., Korner, C. J., Gereige, D., Windels, D., Arnold, A., Kuiper, M., Vazquez, F., Pooggin, M., and Heinlein, M. (2011). Specific impact of tobamovirus infection on the *Arabidopsis* small RNA profile. *PLoS ONE* 6, e19549. doi:10.1371/journal.pone.0019549
- Huang, Y., Ji, L., Huang, Q., Vassilyev, D. G., Chen, X., and Ma, J. B. (2009). Structural insights into mechanisms of the small RNA methyltransferase HEN1. *Nature* 461, 823–827.
- Kim, S., Yang, J. Y., Xu, J., Jang, I. C., Prigge, M. J., and Chua, N. H. (2008). Two cap-binding proteins CBP20 and CBP80 are involved in processing primary microRNAs. *Plant Cell Physiol.* 49, 1634–1644.
- Kozomara, A., and Griffiths-Jones, S. (2011). miRBase: integrating microRNA annotation and deep-sequencing data. *Nucleic Acids Res.* 39, D152–D157.
- Kurihara, Y., and Watanabe, Y. (2004). *Arabidopsis* micro-RNA biogenesis through Dicer-like 1 protein functions. *Proc. Natl. Acad. Sci. U.S.A.* 101, 12753–12758.
- Laubinger, S., Sachsenberg, T., Zeller, G., Busch, W., Lohmann, J. U., Ratsch, G., and Weigel, D. (2008). Dual roles of the nuclear cap-binding complex and SERRATE in pre-mRNA splicing and microRNA processing in *Arabidopsis thaliana*. *Proc. Natl. Acad. Sci. U.S.A.* 105, 8795–8800.
- Li, H., and Durbin, R. (2010). Fast and accurate long-read alignment with Burrows-Wheeler transform. *Bioinformatics* 26, 589–595.
- Li, Y., Li, C., Ding, G., and Jin, Y. (2011). Evolution of MIR159/319 microRNA genes and their post-transcriptional regulatory link to siRNA pathways. *BMC Evol. Biol.* 11, 122. doi:10.1186/1471-2148-11-122
- Llave, C., Xie, Z., Kasschau, K. D., and Carrington, J. C. (2002). Cleavage of Scarecrow-like mRNA targets directed by a class of *Arabidopsis* miRNA. *Science* 297, 2053–2056.
- Llobes, D., Rallapalli, G., Schmidt, D. D., Martin, C., and Clarke, J. (2006). SERRATE: a new player on the plant microRNA scene. *EMBO Rep.* 7, 1052–1058.
- Nag, A., King, S., and Jack, T. (2009). miR319a targeting of TCP4 is critical for petal growth and development in *Arabidopsis*. *Proc. Natl. Acad. Sci. U.S.A.* 106, 22534–22539.
- Palatnik, J. F., Allen, E., Wu, X., Schommer, C., Schwab, R., Carrington, J. C., and Weigel, D. (2003). Control of leaf morphogenesis by microRNAs. *Nature* 425, 257–263.
- Palatnik, J. F., Wollmann, H., Schommer, C., Schwab, R., Boisbouvier, J., Rodriguez, R., Warthmann, N., Allen, E., Dezulian, T., Huson, D., Carrington, J. C., and Weigel, D. (2007). Sequence and expression differences underlie functional specialization of *Arabidopsis* microRNAs miR159 and miR319. *Dev. Cell* 13, 115–125.
- Pant, B. D., Musialak-Lange, M., Nuc, P., May, P., Buhtz, A., Kehr, J., Walther, D., and Scheible, W. R. (2009). Identification of nutrient-responsive *Arabidopsis* and rapeseed microRNAs by comprehensive real-time polymerase chain reaction profiling and small RNA sequencing. *Plant Physiol.* 150, 1541–1555.
- Papdi, C., Abraham, E., Joseph, M. P., Popescu, C., Koncz, C., and Szabados, L. (2008). Functional identification of *Arabidopsis* stress regulatory genes using the controlled cDNA overexpression system. *Plant Physiol.* 147, 528–542.
- Park, M. Y., Wu, G., Gonzalez-Sulser, A., Vaucheret, H., and Poethig, R. S. (2005). Nuclear processing and export of microRNAs in *Arabidopsis*. *Proc. Natl. Acad. Sci. U.S.A.* 102, 3691–3696.
- Park, W., Li, J., Song, R., Messing, J., and Chen, X. (2002). Carpel factory, a Dicer homolog, and HEN1, a novel protein, act in microRNA metabolism in *Arabidopsis thaliana*. *Curr. Biol.* 12, 1484–1495.
- Reinhart, B. J., Weinstein, E. G., Rhoades, M. W., Bartel, B., and Bartel, D. P. (2002). MicroRNAs in plants. *Genes Dev.* 16, 1616–1626.
- Reyes, J. L., and Chua, N. H. (2007). ABA induction of miR159 controls transcripts levels of two MYB factors during *Arabidopsis* seed germination. *Plant J.* 49, 592–606.
- Schommer, C., Palatnik, J. F., Aggarwal, P., Chételat, A., Cubas, P., Farmer, E. E., Nath, U., and Weigel, D. (2008). Control of jasmonate biosynthesis and senescence by miR319 targets. *PLoS Biol.* 6, e230. doi:10.1371/journal.pbio.0060230
- Sobala, A., and Hutvagner, G. (2011). Transfer RNA-derived fragments: origins, processing, and functions. *Wiley Interdiscip. Rev. RNA* 2, 853–862.
- Szarzynska, B., Sobkowiak, L., Pant, B. D., Balazadeh, S., Scheible, W. R., Mueller-Roeber, B., Jarmolowski, A., and Szweykowska-Kulinska, Z. (2009). Gene structures and processing of *Arabidopsis thaliana* HYL1-dependent pri-miRNAs. *Nucleic Acids Res.* 37, 3083–3093.
- Taft, R. J., Glazov, E. A., Lassmann, T., Hayashizaki, Y., Carninci, P., and Mattick, J. S. (2009). Small RNAs derived from snoRNAs. *RNA* 15, 1233–1240.

- Valen, E., Preker, P., Andersen, P. R., Zhao, X., Chen, Y., Ender, C., Dueck, A., Meister, G., Sandelin, A., and Jensen, T. H. (2011). Biogenic mechanisms and utilization of small RNAs derived from human protein-coding genes. *Nat. Struct. Mol. Biol.* 18, 1075–1082.
- Vazquez, F., Blevins, T., Ailhas, J., Boller, T., and Meins, F. Jr. (2008). Evolution of *Arabidopsis* MIR genes generates novel microRNA classes. *Nucleic Acids Res.* 36, 6429–6438.
- Vazquez, F., Gascioli, V., Cr  t  , P., and Vaucheret, H. (2004). The nuclear dsRNA binding protein HYL1 is required for microRNA accumulation and plant development, but not posttranscriptional transgene silencing. *Curr. Biol.* 14, 346–351.
- Weigel, D., Ahn, J. F., Blazquez, M. A., Borevitz, J. O., Christensen, S. K., Fankhauser, C., Ferrandiz, C., Karadailsky, I., Malancharuvil, E. J., Neff, M. M., Nguyen, J. T., Sato, S., Wang, Z. Y., Xia, Y., Dixon, R. A., Harrison, M. J., Lamb, C. J., Yanofsky, M. F., and Chory, J. (2000). Activation tagging in *Arabidopsis*. *Plant Physiol.* 122, 1003–1014.
- Yang, L., Liu, Z., Lu, F., Dong, A., and Huang, H. (2006a). SERRATE is a novel nuclear regulator in primary microRNA processing in *Arabidopsis*. *Plant J.* 47, 841–850.
- Yang, Z., Ebright, Y. W., Yu, B., and Chen, X. (2006b). HEN1 recognizes 21–24 nt small RNA duplexes and deposits a methyl group onto the 2' OH of the 3' terminal nucleotide. *Nucleic Acids Res.* 34, 667–675.
- Yu, B., Bi, L., Zheng, B., Ji, L., Chevalier, D., Agarwal, M., Ramachandran, V., Li, W., Lagrange, T., Walker, J. C., and Chen, X. (2008). The FHA domain proteins DAWDLE in *Arabidopsis* and SNIP1 in humans act in small RNA biogenesis. *Proc. Natl. Acad. Sci. U.S.A.* 105, 10073–10078.
- Zhang, W., Gao, S., Zhou, X., Xia, J., Chellappan, P., Zhou, X., Zhang, X., and Jin, H. (2010). Multiple distinct small RNAs originate from the same microRNA precursors. *Genome Biol.* 11, R81.
- Zhou, H., Zhang, Q., Zhang, J., Ni, F., Liu, C., and Qi, Y. (2010). DNA methylation mediated by a microRNA pathway. *Mol. Cell* 38, 465–475.

Conflict of Interest Statement: The authors declare that the research was conducted in the absence of any commercial or financial relationships that could be construed as a potential conflict of interest.

Received: 21 November 2011; accepted: 25 February 2012; published online: 19 March 2012.

Citation: Sobkowiak L, Karlowski W, Jarmolowski A and Szweykowska-Kulinska Z (2012) Non-canonical processing of *Arabidopsis* pri-miR319a/b/c generates additional microRNAs to target one RAP2.12 mRNA isoform. *Front. Plant Sci.* 3:46. doi: 10.3389/fpls.2012.00046

This article was submitted to *Frontiers in Plant Genetics and Genomics*, a specialty of *Frontiers in Plant Science*.

Copyright © 2012 Sobkowiak, Karlowski, Jarmolowski and Szweykowska-Kulinska. This is an open-access article distributed under the terms of the Creative Commons Attribution Non Commercial License, which permits non-commercial use, distribution, and reproduction in other forums, provided the original authors and source are credited.

APPENDIX

List of all sRNA sequences which match the miR319 primary transcripts

pri-miR_id start:end_position strand raw_counts miR_id

ath-MIR319a 48:69 + 8 miR319a.2*
ath-MIR319a 110:132 + 16 miR319a.2
ath-MIR319a 152:171 + 6
ath-MIR319a 154:169 + 5
ath-MIR319a 154:174 + 90 miR319a
ath-MIR319a 155:173 + 5

ath-MIR319b 3:21 + 5
ath-MIR319b 3:23 + 213 miR319b*
ath-MIR319b 4:22 + 10
ath-MIR319b 4:23 + 35
ath-MIR319b 4:24 + 6
ath-MIR319b 48:69 + 8 miR319b.2*
ath-MIR319b 108:122 + 8
ath-MIR319b 108:123 + 7
ath-MIR319b 108:124 + 10
ath-MIR319b 108:125 + 22
ath-MIR319b 108:126 + 21
ath-MIR319b 108:127 + 73
ath-MIR319b 108:128 + 538 miR319b.2
ath-MIR319b 108:129 + 132
ath-MIR319b 108:130 + 98
ath-MIR319b 108:131 + 11
ath-MIR319b 109:129 + 8
ath-MIR319b 152:167 + 5
ath-MIR319b 152:172 + 90 miR319b
ath-MIR319b 153:171 + 5

ath-MIR319c 126:146 + 16 miR319c.2
ath-MIR319c 170:185 + 5
ath-MIR319c 170:190 + 31 miR319c

